Article

Screening the Pathogen Box to Discover and Characterize New Cruzain and *Tbr*CatL Inhibitors

Thales do Valle Moreira [1,†], Luan Carvalho Martins [1,†], Lucas Abreu Diniz [1], Talita Cristina Diniz Bernardes [1], Renata Barbosa de Oliveira [2] and Rafaela Salgado Ferreira [1,*]

[1] Molecular Modeling and Drug Design Laboratory, Department of Biochemistry and Immunology, Institute of Biological Sciences, Federal University of Minas Gerais, 6627, Antônio Carlos Avenue, Belo Horizonte 31270-901, MG, Brazil
[2] Pharmaceutical Products Department, Federal University of Minas Gerais, 6627, Antônio Carlos Avenue, Belo Horizonte 31270-901, MG, Brazil
* Correspondence: rafaelasf@icb.ufmg.br
† These authors contributed equally to this work.

Abstract: Chagas disease and Human African Trypanosomiasis, caused by *Trypanosoma cruzi* and *T. brucei*, respectively, pose relevant health challenges throughout the world, placing 65 to 70 million people at risk each. Given the limited efficacy and severe side effects associated with current chemotherapy, new drugs are urgently needed for both diseases. Here, we report the screening of the Pathogen Box collection against cruzain and *Tbr*CatL, validated targets for Chagas disease and Human African Trypanosomiasis, respectively. Enzymatic assays were applied to screen 400 compounds, validate hits, determine IC_{50} values and, when possible, mechanisms of inhibition. In this case, 12 initial hits were obtained and ten were prioritized for follow-up. IC_{50} values were obtained for six of them (hit rate = 1.5%) and ranged from 0.46 ± 0.03 to 27 ± 3 μM. MMV687246 was found to be a mixed inhibitor of cruzain ($K_i = 57 \pm 6$ μM) while MMV688179 was found to be a competitive inhibitor of cruzain with a nanomolar potency ($K_i = 165 \pm 63$ nM). A putative binding mode for MMV688179 was obtained by docking. The six hits discovered against cruzain and *Tbr*CatL are of great interest for further optimization by the medicinal chemistry community.

Keywords: Chagas disease; cruzain; screening; drug discovery; small molecule inhibitors; Pathogen Box

1. Introduction

Despite being described over a hundred years ago, Chagas Disease (CD, also American Trypanosomiasis) and Human African Trypanosomiasis (HAT, also sleeping sickness) are still relevant public health problems [1]. While CD accounts for a burden of 546,000 Disability-Adjusted Life Years (DALY) [2] and threatens circa 70 million people with a risk of infection [3], HAT causes a burden of 560,000 DALY [2] and threatens circa 65 million people [4,5]. Moreover, global warming has been shifting CD transmission zones, raising worries in previously transmission-free areas [6], whereas business, commerce, and migration have spread CD prevalence to all inhabited continents except Africa [7]. Addressing the global problem posed by these Neglected Tropical Diseases (NTD) is a costly, long-term investment, as making a novel drug into the market is a billionaire enterprise [8]. Nevertheless, the socio-economic benefits of improving the CD and HAT scenarios are certain [9].

Available treatments are suboptimal for both diseases. Benznidazole and Nifurtimox, the current chemotherapeutic options for CD, are only effective in the acute phase and are associated with significant adverse effects, which include gastric and neurological disorders [3,10–13]. Moreover, it was shown that chronic asymptomatic patients have no clinical benefit on their cardiac condition after Benznidazole therapy [14]. Likewise, HAT chemotherapeutic resources are highly toxic and low-efficacy drugs [4], which leave

many patients untreated, still infected with the parasite. Suramin and Pentamidine are only useful in the early stages of the disease and are associated with severe side effects, including lethal hypoglycemia for Pentamidine [15,16]. Melarsoprol is restricted to the late-stage HAT mainly because 1 out of 10 treated patients will suffer from lethal, reactive encephalopathy [17,18]. Eflornithine is better tolerated than Melarsoprol, but it has to be administered by daily injections [19]. Nifurtimox-eflornithine combination therapy (NECT) presents safety advantages, but still has similar efficacy to eflornithine monotherapy [20,21]. Cost, severe side effects, and complex mode of administration limit Eflornithine mostly to a second-line, late-state treatment [19,22]. Fexinidazole is an oral treatment for late-stage HAT caused by the *T. b. gambiense* strain, with efficacy similar to NECT [23–25], and is currently under clinical trials for use against the *T. b. rhodesiense* strain [26]. Therefore, a safe orally administered drug, active against both *T. b. gambiense* and *T. b. rhodesiense,* and either in early or late stages is highly demanded [4,11,12,16].

Cruzain, a cysteine protease of *Trypanosoma cruzi*, is a validated [11,27–29] and well-explored pharmacological target (see [30] for a recent review). Cruzain is the truncated, recombinant-expressed cruzipain 1, part of a multigenic family comprising of four sub-types of cruzipains [31]. *Tbr*CatL, a homologous protease from *Trypanosoma brucei,* is also a validated target for discovering trypanocidal compounds [32,33]. Cruzain is expressed throughout the whole life cycle of the parasite [34] and is involved in several vital processes such as replication [35], cellular invasion [36,37], and modulation of macrophage response [38]. *Tbr*CatL might be relevant for the parasite to cross the blood-brain barrier [39], although this subject is still a matter of dispute [40]. Several classes of cruzain inhibitors have been described such as: thiosemicarbazones [41,42], nitrile-based derivatives [43,44], aminoquinolines [45], benzimidazoles [46,47], vinyl sulfones [48,49], analogues of Gallinamide A [50], quinazolines [51], and carbamoyl imidazoles [52]. Likewise, diverse *Tbr*CatL inhibitors have been reported, such as thiosemicarbazones [53], bromoisoxazolines [54], nitriles [55,56], thiazoles and thiazolidines [57,58], triazoles [59], macrocyclic lactams [33], vinyl sulfones [60], vinyl ketones [61], and vinyl esters [62]. Simultaneously investigating the same libraries against these two cysteine proteases can be fruitful due to their similarities, a strategy that has resulted in the description of several inhibitor classes targeting both proteases [11,12,29,42,43,45,60,63,64].

One of the strategies for discovering new lead inhibitors for a target is screening diverse, curated compound sets. For instance, the Medicines for Malaria Venture (MMV) partnership organized the Malaria Box, a compound set for catalyzing NTD research [65]. The Malaria Box was widely screened worldwide, resulting in the discovery of hits against several pathogens and targets [65], including new cruzain and *Tbr*CatL inhibitors [63]. More recently, MMV assembled the Pathogen Box (PB), a compound set targeting a broader scope of parasites (https://www.mmv.org/mmv-open/pathogen-box/about-pathogen-box, accessed on 3 February 2023). PB comprises of 400 drug-like compounds active against parasites that cause NTD and with low-cytotoxic. Some of the molecules originally included in the PB due to in vitro activity against other parasites other than trypanosomatids were later reported to show trypanocidal activity [66,67].

Given the relevance of CD and HAT and the attractiveness of cruzain and *Tbr*CatL as targets, we screened and validated hits from the PB against both enzymes. Out of 400 compounds, we describe six hits with IC_{50} in the low micromolar to nanomolar range against both enzymes, including one competitive inhibitor. These molecules will be very relevant for future medicinal chemistry efforts.

2. Materials and Methods

2.1. Data on the PB Collection

PB data spreadsheets containing chemical structures, SMILES, molecular weight, cLogP and biological activity were retrieved from the Pathogen Box website (www.mmv.org, accessed on 30 May 2020). HepG2 cytotoxicity data (CC_{20} and/or CC_{50}) are also provided

for approximately three-quarters of the compounds. Data on other assays for selected compounds were obtained from the CHEMBL database [68].

2.2. PB Collection Samples

The 400 compounds from the Pathogen Box were supplied in 96-well plates containing 10 mM frozen dimethylsulfoxide (DMSO) solutions. Solid samples of the 10 following compounds were resupplied by Evotec upon request to the MMV: MMV688179, MMV688271, MMV667494, MMV634140, MMV690027, MMV690028, MMV688362, MMV085499, MMV687246, MMV688466, MMV687812, MMV688466, and MMV085499.

2.3. Assays against Cruzain and TbrCatL

Allison Doak and Prof. Brian Shoichet (University of California San Francisco, San Francisco, CA, USA) and Prof. Conor Caffrey (University of California San Diego, San Diego, CA, USA) generously provided recombinant cruzain and *Tbr*CatL, respectively. In vitro activity of proteases cruzain and *Tbr*CatL was assayed as previously described [45,63]. Briefly, enzyme activity was measured by monitoring the cleavage of the fluorogenic substrate Z-Phe-Arg-amidomethylcoumarin (Z-FR-AMC) at 25 °C. Fluorescence was monitored at 340/440 nm (excitation/emission) over 5–7 min in a Synergy2 Biotek plate reader. Unless stated otherwise, assays were performed using 2.5 μM substrate ($K_m = 0.5 \pm 0.1$ μM against cruzain and $K_m = 0.5 \pm 0.1$ μM against *Tbr*CatL [63]) and circa 0.5 nM enzyme in a pH 5.5 buffer composed of 0.1 M sodium acetate buffer, 0.01% Triton X-100, and 1 mM β-mercaptoethanol. DMSO and 1 μM E-64 were employed as negative and positive controls, respectively, in all assays. Two conditions were employed for both enzymes: 10′ pre-incubation of the enzyme in the presence of the compound (10′ inc) and no pre-incubation (0′). Reported values correspond to the mean and standard error of the mean (SEM) and all analyses were performed using GraphPad Prism 6.0.

For the initial screening, compounds were assayed at 5 μM. Compounds were selected for further assays based on the combination of the inhibition observed, novelty, and diversity (see details below). IC_{50} curves were obtained from a non-linear fit of at least seven distinct compound concentrations, in triplicate. Reported IC_{50} values are the mean and SEM of two independent measurements.

To assess the effects of the Triton X-100 concentration on cruzain inhibition, assays were performed using 0.001%, 0.01%, and 0.1% Triton X-100. To evaluate the impact of pre-incubation with bovine serum albumin (BSA), 50 μL of a solution of the compound in the assay buffer containing 0.001% of Triton X-100 was incubated with 4 mg/mL of BSA (Sigma-Aldrich) for 10′ in a 96-well plate. Next, 50 μL of a solution containing circa 2 nM of cruzain in the same buffer was added to each well and incubated for another 10′. Finally, 100 μL of a solution of 5 μM Z-FR-AMC in the same buffer was added to each well and the fluorescence was immediately read. The final compound concentration varies and was selected to be near the compound IC_{50}. When analyzing the effects on the inhibition of the concentration of Triton X-100 and pre-incubation of the compound with BSA, differences higher than 20% were considered [51].

The mechanisms of inhibition were determined using seven substrate concentrations (10 μM, 5 μM, 2.5 μM, 1.25 μM, 625 nM, 312.5 nM, 156 nM) and five inhibitor concentrations (including one concentration close to the compound's IC_{50} value, two concentrations higher and two concentrations lower than the IC_{50}) and in the absence of the compound. Non-linear regression to Michaelis-Menten models and linear regression for the Lineweaver-Burk plot were performed. K_i was estimated by both methods. The effect of the inhibitor concentration on the $K_{m\ app}$ was evaluated using the General Linear F-test.

2.4. Analogue Search

Analogues of MMV688179 were searched in BraCoLi, a diverse database (containing 1176 molecules previously synthesized by Brazilian medicinal chemistry groups as of October 2022) [69] using DataWarrior. FragFP molecular fingerprints were generated for

the entire library and then used to generate a similarity map. The Bemis-Murcko [70] core of MMV688179 was extracted and used as a reference for similarity comparison. Molecules most similar to the core and readily available in our stocks were selected for assays.

2.5. Synthesis and Characterization

The synthesis and characterization of compounds 1–5 [71] and 6–7 [72] were previously reported.

2.6. Molecular Docking

The crystallographic structure of cruzain was obtained from RSCB PDB (ID: 3KKU [73]) and had hydrogens added using PDB2PQR [74] using a model pH of 5.5. The catalytic dyad was modelled as an ionic pair and Glu208 was modelled in the deprotonated state. MMV688179 was obtained from ChemBL and the most common protomer at pH 5.5, predicted using ChemAxon MarvinSketch (Marvin version 21.15.0, ChemAxon (https://www.chemaxon.com, accessed on 8 December 2022), was the +2 protomer. MMV688179 geometry was optimized at ab initio level using HF/6-31G* in Psi4 [75]. Docking was performed in AutoDock Vina 1.2.3 [76]. The grid was centered at the center of mass of the crystallographic ligand of the protein and exhaustiveness was set to 32. All other parameters for AutoDock Vina were kept at default values. Ten poses were generated and visually inspected for complementarity between the ligand and the binding site, the presence of hydrogen bonds and polar interactions, and the absence of strained torsional angles.

3. Results

To assess potential hits against cruzain and *Tbr*CatL, we initially screened the 400 compounds in the PB library at 5 μM against both enzymes (Figure 1). Overall, the dispersion of the results was low as shown by the mean Standard Deviation (SD) of 5.8 percentage points (pp)% over all measurements (N = 1600). Only four compounds (1%: MMV667494, MMV676881, MMV688179, MMV688271) inhibited cruzain or *Tbr*CatL by at least 60%, while 12 compounds (3%: MMV085499, MMV634140, MMV667494, MMV676881, MMV687246, MMV687812, MMV688179, MMV688271, MMV688362, MMV688466, MMV690027, MMV690028) inhibited either enzyme by at least 40% (Figure 2, see also Supplementary Material 1).

Hits were chosen for follow-up based on the combined analysis of their novelty concerning known inhibitors, chemical diversity within the set, and potency in the initial screening. We initially considered for further investigation the 12 compounds that inhibited either cruzain or *Tbr*CatL by at least 40% either without pre-incubation or after 10′ pre-incubation (Figure 3, Table 1). Compound MMV676881 fully inhibited cruzain and *Tbr*CatL both with and without pre-incubation, but it was deprioritized as it is a well-known purine-nitrile cruzain inhibitor [43]. The arylamidine MMV688179 also completely inhibited cruzain both without and with incubation, although inhibition towards *Tbr*CatL was more modest (0′: (50 ± 5)%; 10′ inc: (58 ± 44)%, Table 1). MMV688271, an isomer of MMV688179, inhibited the enzymes to a lesser extent and was not prioritized for follow-up. Similarly, among the structurally related quinolines MMV667494 and MMV634140, the former was prioritized due to its higher potency against *Tbr*CatL after 10′ incubation $((73 \pm 1)$% vs. (42 ± 3)%). MMV690028 was prioritized because of its *Tbr*CatL inhibition $(49 \pm 4$% without pre-incubation). MMV690027 was deprioritized because of its low cruzain inhibition $((6 \pm 2)$% without pre-incubation; (0 ± 6)% after 10′ pre-incubation) and because it was supplied as a racemic mixture. MMV085499 and MMV687246 were prioritized based on the *Tbr*CatL inhibition results after pre-incubation $((46 \pm 5)$% and (49 ± 4)%, respectively). MMV688179, MMV688271, and MMV688362 have been previously assayed against *T. cruzi* and *T. brucei* and showed IC$_{50}$ between 0.2 μM and 14 μM [77,78] (Table S1). Surprisingly, the screen also revealed compounds that increased enzyme activity. In the presence of the pyridinylthiazole MMV676409 (Table S2), we observed higher initial velocities of substrate cleavage, up to 8-fold higher in comparison to the DMSO control (*Tbr*CatL 10′ inc). Compound MMV676512 (Table S2), which is structurally similar to MMV676409,

showed a similar, but less pronounced effect (a 2-fold increase in *Tbr*CatL velocity after 10′ pre-incubation). Thus, we also selected compounds MMV676409 and MMV676512 for further investigation.
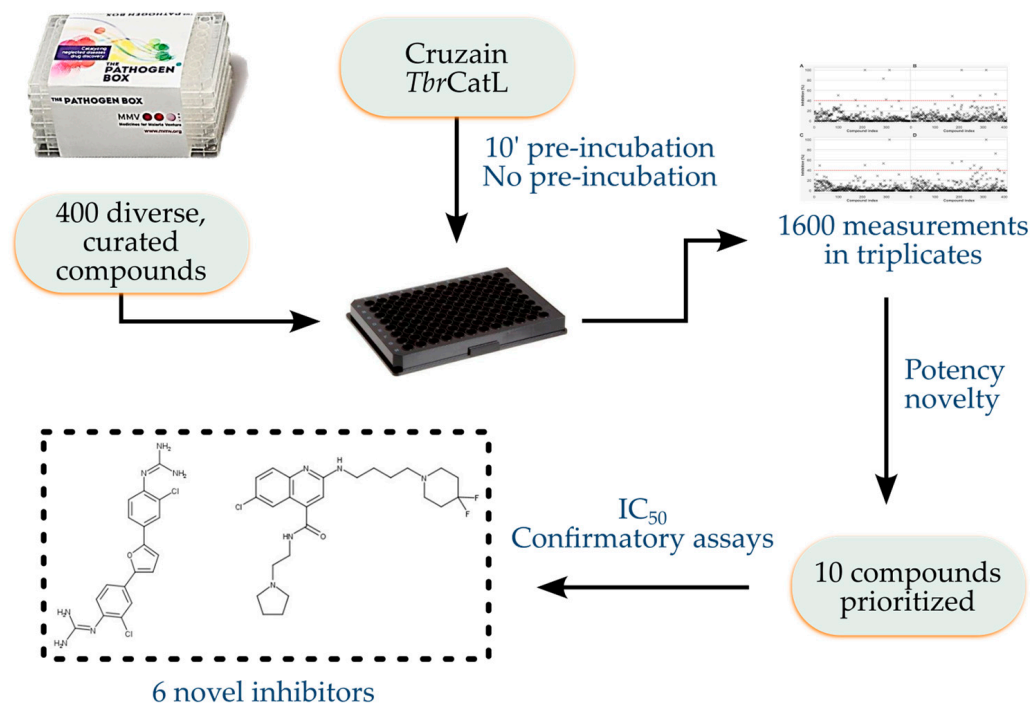

Figure 1. Workflow of the study. The 400 compounds of the Pathogen Box set were assayed for inhibition of cruzain and *Tbr*CatL. The 1600 inhibition measurements were analyzed and compounds inhibiting >40% of the enzyme activity against either cruzain or *Tbr*CatL were considered for prioritization. Ten compounds were prioritized and six of them were confirmed to be inhibitors with IC_{50} ranging from 0.46 ± 0.03 to 27 ± 3 μM.

Next, we evaluated the compounds selected from the screening, at a concentration of 100 μM, to confirm their activity using solid samples provided by Evotec (Table 1). Assays for MMV676409 and MMV676512 showed no increase in the enzyme velocity under varying compound concentrations, suggesting that these compounds are not activators of cruzain (Table S2). Failing in reproducing inhibitions observed in the screen during confirmatory assays is common, so we believe that the lack of activation is not surprising [63]. More specifically, activators have also been observed in an HTS against cruzain but were not confirmed in follow-up assays [79]. MMV085499 is fluorescent at 330/440 nm, thus resulting in interference with the assay and could not be further evaluated. MMV667494 results were not reproducible, as no *Tbr*CatL inhibition was observed in the confirmatory assays. This compound was modestly potent against cruzain after pre-incubation ((70 ± 3)% inhibition), but not potent enough for IC_{50} determination. The remaining six compounds inhibited either or both enzymes to a 90–100% extent, and we determined their IC_{50} against both enzymes with and without pre-incubation (Table 1, see also Figure S1).

Overall, IC_{50} values determined with and without 10′ pre-incubation were similar (up to 2-fold change for MMV687246 against cruzain), suggesting that none of the compounds is a time-dependent inhibitor. Furthermore, because none of these compounds bears electrophilic moieties, the inhibition likely is a fast-reversible, non-covalent one. Therefore, the IC_{50} and K_i values can capture the potency of these compounds. In addition, potencies towards cruzain and *Tbr*CatL were similar for all compounds, except for MMV688179, which was the most potent cruzain inhibitor (IC_{50} 0.46 ± 0.03 μM 0′ and 0.53 ± 0.03 10′ inc) but had 10-fold higher IC_{50} against *Tbr*CatL (IC_{50} = 4 ± 1 μM 0′ and 5 ± 2 uM 10′ inc).

MMV688362 was the most potent *Tbr*CatL inhibitor (IC$_{50}$ 2.9 ± 0.8 μM 0′ and 2.3 ± 0.1 μM 10′ inc).

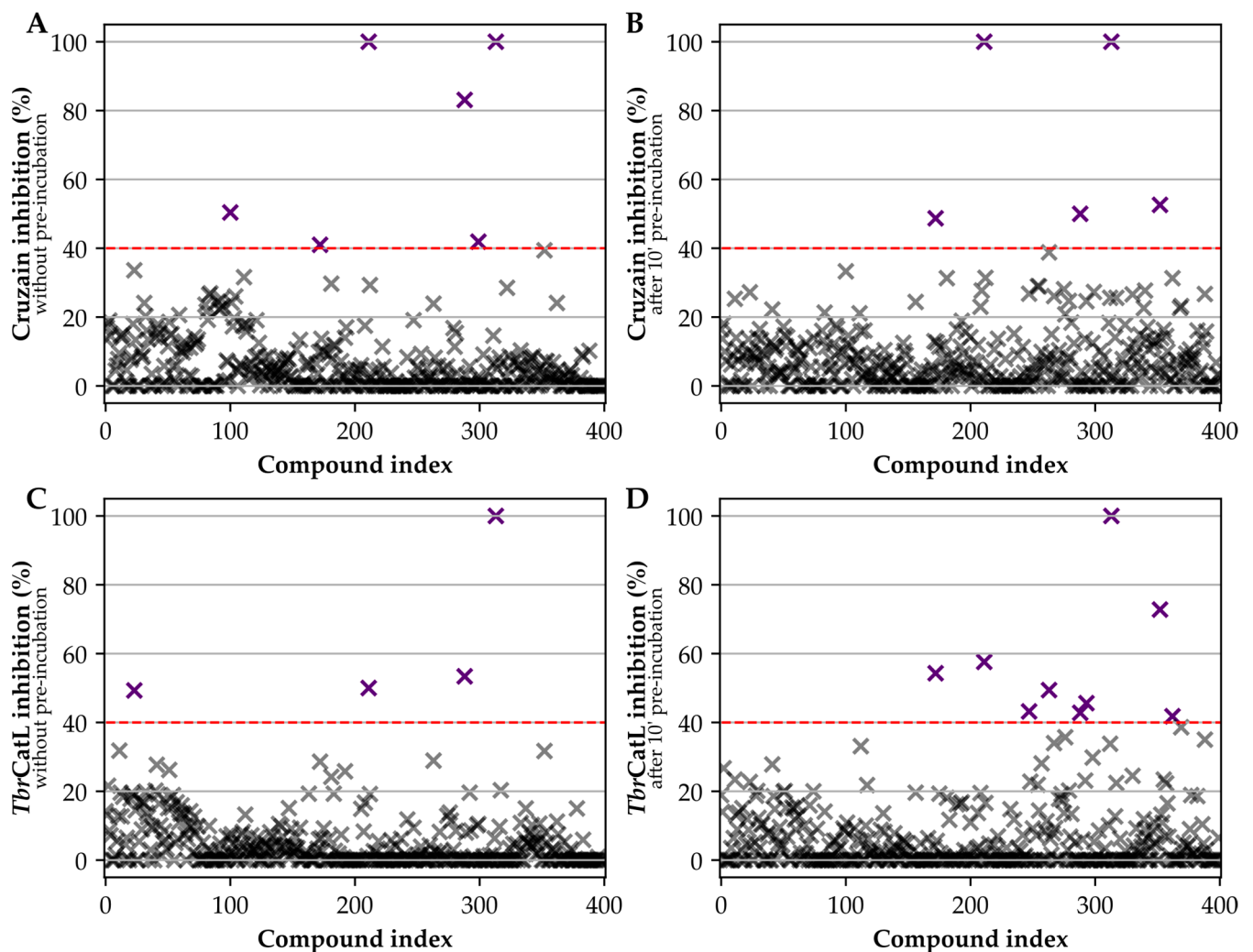**Figure 2.** Scatter plots of mean inhibitions observed in the screening at 5 μM. (**A**) Inhibition of cruzain without pre-incubation. (**B**) Inhibition of cruzain after 10′ pre-incubation. (**C**) Inhibition of *Tbr*CatL without pre-incubation. (**D**) Inhibition of *Tbr*CatL after 10′ pre-incubation. Values below 40% are depicted as semi-transparent grey crosses. Values above 40% are depicted as purple crosses.

To investigate if inhibition was due to colloidal aggregation, a common cause of unspecific enzyme inhibition in in vitro assays [79], we employed two well-established experiments: the comparison of percentages of inhibition at varying Triton X-100 concentrations and the effect of compound pre-incubation with BSA on the percentage of inhibition. Triton X-100 disrupts small molecule aggregates, so a large reduction in the inhibition observed in high Triton concentration (0.01 or 0.1%) when compared to a low concentration (0.001%) suggests the compound aggregates [80]. Pre-incubating a compound that aggregates with BSA saturates the protein-binding capacity of the aggregate. Therefore, if pre-incubating a compound with BSA reduces the inhibition, it suggests that the compound aggregates [81]. For MMV688362 and MMV687812 we observed some reduction in the inhibition upon the pre-incubation of the compound with BSA and upon a 10-fold increase in the concentration of Triton X-100, respectively (Table S3). It is worth noting, however, that pre-incubation of MMV687812 with BSA did not reduce the inhibition of cruzain. While these two compounds might possess some aggregation properties near the IC$_{50}$,

overall the results do not suggest aggregation. Importantly, results for MMV688179, the most potent cruzain inhibitor, do not suggest aggregation properties near the IC_{50}.
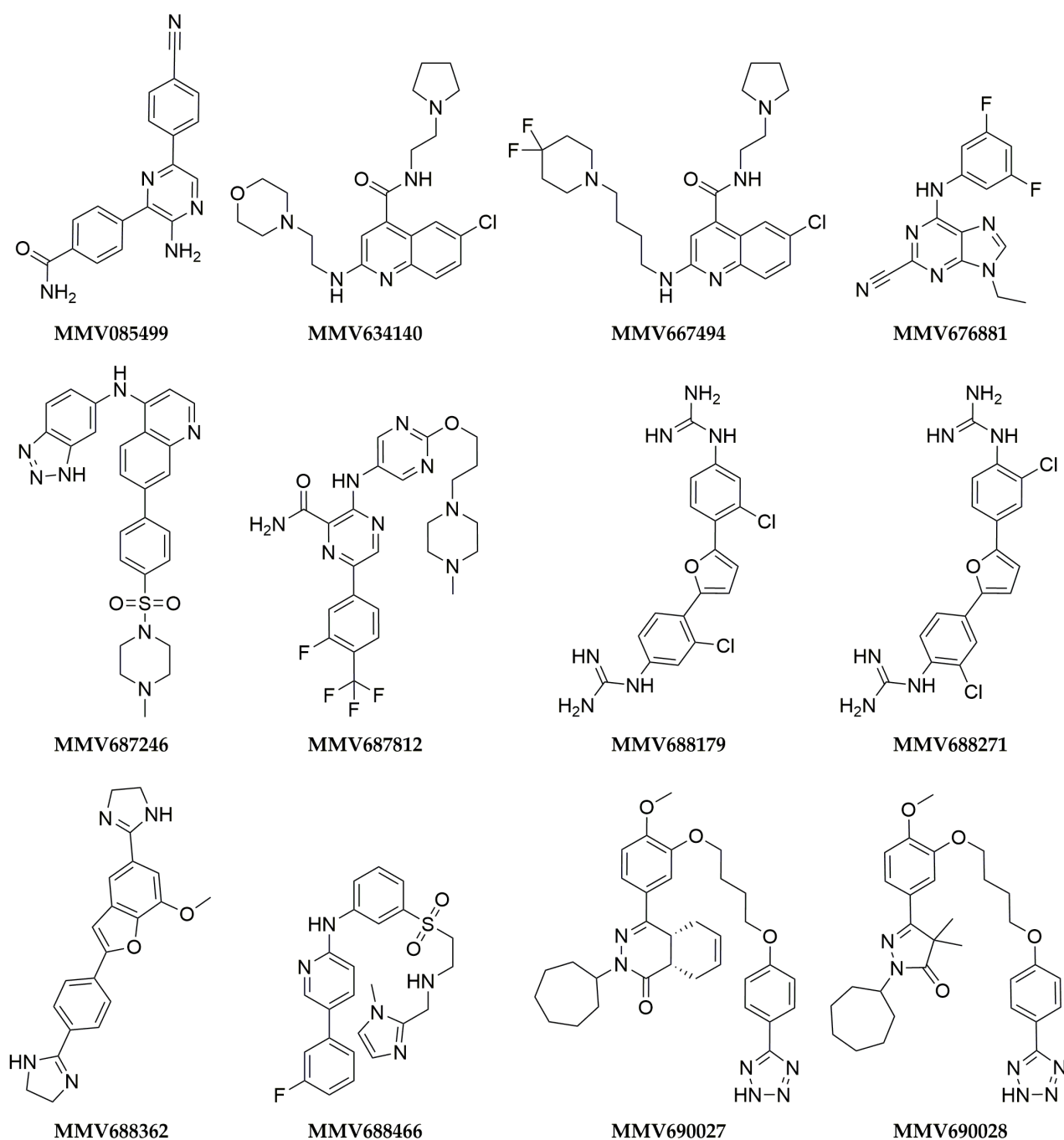

Figure 3. Structures of compounds inhibiting cruzain or *Tbr*CatL by at least 40% in the initial screening at 5 μM.

Inhibition mechanisms against cruzain could be determined for MMV688179 and MMV687246 (Figure 4). For MMV687246 a mixed inhibition was observed with an α value slightly smaller than 1 (α = 0.7 ± 0.2) and a K_i = 57 ± 6 μM (Figure 4A). The lack of substrate competition is also suggested by the Lineweaver-Burk plot (Figure 4B). Accordingly, analysis of the K_{mapp} at varying concentrations of MMV687246 suggests that the concentration of MMV687246 does not affect the K_{mapp} (general linear F-test, *p*-value = 0.1701, Figure 4C). For MMV688179 we clearly observed competition with the substrate, based on

the combined analysis of the Michaelis-Menten (Figure 4D) and Lineweaver-Burk plots (Figure 4E). The K_i was estimated to be 165 ± 63 nM from the non-linear regression of the Michaelis-Menten competitive model and 206 nM from the linear regression of K_{mapp} (Figure 4F), for which the hypothesis of the slope to be 0 can be rejected (general linear F-test, *p*-value < 0.0001).

Table 1. *Tbr*CatL and cruzain inhibition by hits prioritized after the initial screening of the Pathogen Box.

Compound	Inhibition at 5 µM (Mean ± SEM %) [a]				Inhibition at 100 µM (Mean ± SEM %) [b]				IC$_{50}$ (µM ± SEM %) [c]			
	*Tbr*CatL		Cruzain		*Tbr*CatL		Cruzain		*Tbr*CatL		Cruzain	
	0′	10′ inc	0′	10′ inc	0′	10′ inc	0′	10′ inc	0′	10′ inc	0′	10′ inc
MMV085499	12 ± 8	46 ± 5	2 ± 3	25 ± 4	26 ± 18	0 ± 0	0 ± 0	0 ± 0	ND	ND	ND	ND
MMV634140	11 ± 1	42 ± 3	24 ± 1	31 ± 3	ND	ND	ND	ND	ND	ND	ND	ND
MMV667494	31 ± 5	73 ± 1	40 ± 1	53 ± 1	0 ± 0	11 ± 8	0 ± 0	70 ± 3	ND	ND	ND	ND
MMV676881	100 ± 0	100 ± 2	100 ± 2	100 ± 1	ND	ND	ND	ND	ND	ND	ND	ND
MMV687246	29 ± 1	49 ± 4	24 ± 3	39 ± 3	92 ± 6	99 ± 1	72 ± 1	92 ± 3	9 ± 3	4.2 ± 0.6	14 ± 5	10 ± 2
MMV687812	11 ± 3	5 ± 1	41 ± 2	27 ± 0	90 ± 2	93 ± 0	100 ± 0	95 ± 0	3.45 ± 0.05	3.6 ± 0.3	2.2 ± 0.3	2.6 ± 0.03
MMV688179	50 ± 3	58 ± 25	98 ± 2	100 ± 0	100 ± 0	100 ± 0	100 ± 0	100 ± 0	4 ± 1	5 ± 2	0.46 ± 0.03	0.53 ± 0.03
MMV688271	53 ± 5	43 ± 1	83 ± 10	50 ± 4	ND	ND	ND	ND	ND	ND	ND	ND
MMV688362	9 ± 1	43 ± 4	19 ± 1	27 ± 3	100 ± 0	100 ± 0	100 ± 0	100 ± 0	2.9 ± 0.8	2.3 ± 0.1	4.2 ± 0.6	2.35 ± 0.02
MMV688466	29 ± 2	54 ± 8	41 ± 2	49 ± 5	96 ± 3	100 ± 0	58 ± 27	98 ± 1	4 ± 1	11 ± 4	9 ± 1	25 ± 6
MMV690027	6 ± 2	0 ± 6	50 ± 5	33 ± 2	ND	ND	ND	ND	ND	ND	ND	ND
MMV690028	49 ± 4	23 ± 4	34 ± 8	27 ± 4	100 ± 0	88 ± 3	100 ± 0	100 ± 0	18 ± 7	27 ± 3	10 ± 3	13 ± 5

ND = not determined [a]: mean over three independent measurements, values larger than 100% were represented as 100% and values lower than 0% were represented as 0%. [b]: mean over two independent experiments, in triplicates. [c]: mean over two independent experiments, in triplicates, spanning at least seven compound concentrations.

Motivated by the high potency and competitive mechanism of MMV688179 against cruzain, we sought to obtain preliminary SAR data on this scaffold. We used a similarity search to find analogues bearing a similar diphenylfurane core in an in-house library (Bra-CoLi) and obtained seven analogues that were available in our stocks (Figure 5, Table S4). Unfortunately, we were unable to test most compounds, due to issues with solubility and fluorescence at 330/440 nm. The few compounds tested were much less potent than MMV688179, causing inhibitions of $(57 \pm 4)\%$ and $(65 \pm 4)\%$ at 100 µM (Table S4).

Due to the competitive mechanism and the high potency of MMV688179, we employed molecular docking to propose a binding mode for this molecule. Overall, the ten docking poses were similar and the best-scored one was selected by visual inspection as the possible binding mode of MMV688179. In this binding pose, one of the protonated guanidines is buried in the S2 subsite and an ion-ion interaction with Glu208 is suggested. The other protonated guanidine forms hydrogen bonds with the main chain of residues Gly20 and Cys22, both at the S1 subsite (Figure 6). In addition to these polar interactions, the docking pose spans over a large part of the catalytic cleft, with good spatial complementarity to the protein site, which indicates a high number of van der Waals interactions and is in line with the high potency and competitive mechanism. No interactions were observed for the chlorine atoms, which would rationalize the similar, although slightly lower, inhibition of MMV688271 in the initial screen. In addition, the docking pose suggests the furan ring acts as a linker. However, further studies will be required to shed light on the SAR of MMV688179.
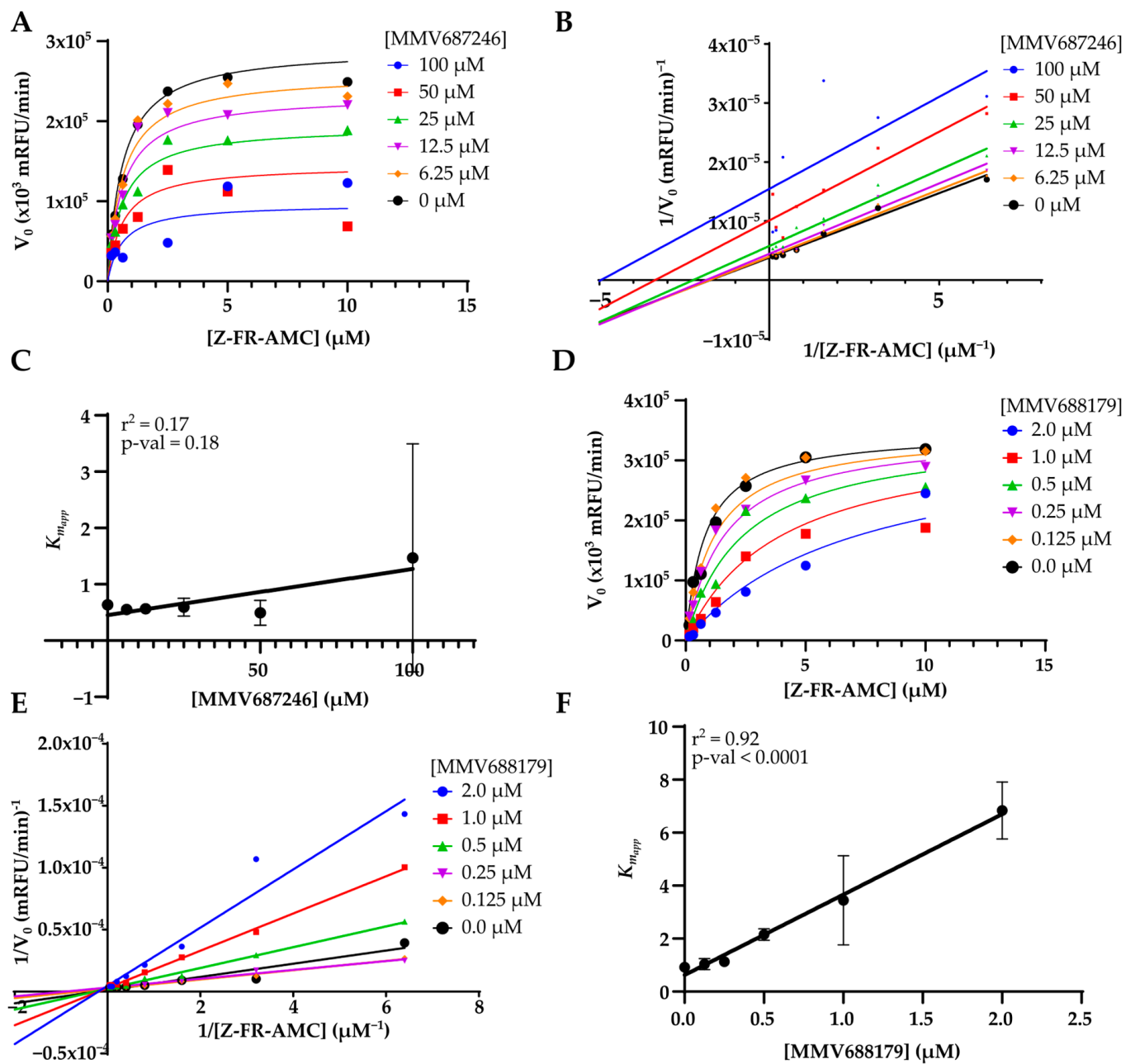
Figure 4. Plot of the assays to determine the mechanism of inhibition of MMV687246 and MM688179. (**A**) Michaelis-Menten plot for MMV687246. The curves correspond to the fitting of a mixed-model of inhibition to data. (**B**) Lineweaver-Burk plot for MMV687246. (**C**) Plot of the K_{mapp} for varying MMV687246 concentrations. Points are the mean of two replicas. *p*-val is the 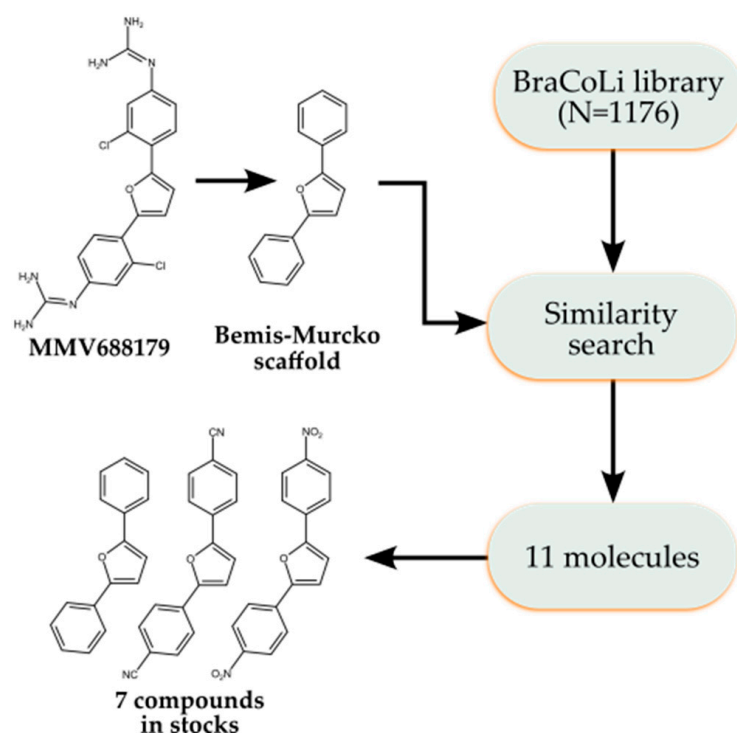*p*-value of the general linear F-test. (**D**) Michaelis-Menten plot for MMV688179. The curves correspond to the fitting of a mixed-model of inhibition to data. (**E**) Lineweaver-Burk plot for MMV688179. (**F**) Plot of the K_{mapp} for varying MMV688179 concentrations. Points are the mean of two replicas. *p*-val is the *p*-value of the general linear F-test.

Figure 5. Workflow for searching for MMV688179 analogues. The Bemis-Murcko scaffold of MMV688179 was calculated and used as a reference for the similarity search of analogues in the BraCoLi dataset. Here, 11 molecules were selected and seven of them were in stock.
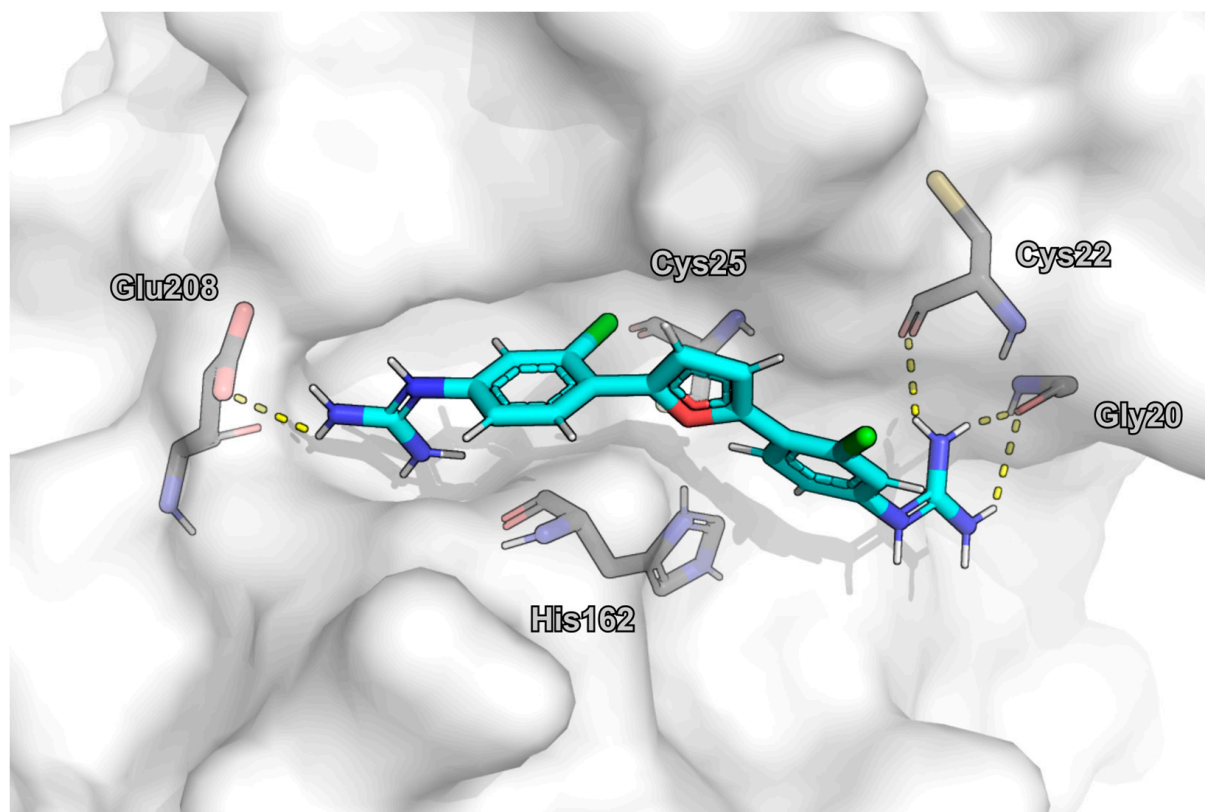
Figure 6. Docking pose of MMV688179 bound to cruzain's active site. Figure prepared in PyMol 2.4.0.

4. Discussion

Regarding NTD drug discovery, phenotypic approaches seemed to have been overshadowed by target-based ones over the second half of the 20th century. Their apparent historic contrast has then evolved and merged into complementarity [82]. First-in-class compounds are often discovered in phenotypic approaches whereas further molecular lead optimization follows target-based campaigns. Starting from phenotypical hits, however, may lead to challenges in optimization steps [83]. The MMV chemical boxes are a relevant contribution in that sense, providing phenotypically validated molecules to groups for evaluation in additional phenotypic assays or target-based approaches. The PB compounds are active against a wide range of pathogens but chiefly against *Plasmodium* (125 antimalarials, 33% of the tested molecules), *Mycobacterium* (116, 30%), and kinetoplastids (70, 18%), with the remaining 19% being active against other pathogens [66,77]. Most of the cysteine protease inhibitors discovered in our study have previously shown activity against kinetoplastids. Thus, we contribute toward the deconvolution of the targets related to their trypanocidal activity. For instance, MMV688179 is trypanocidal with an EC_{50} of 27 μM against *T. cruzi* [84], and given the IC_{50} against cruzain we report here, cruzain inhibition is possibly related to its trypanocidal activity. This may also be true for MMV688362 (EC_{50} against *T. cruzi* reported on PB: 13 μM). Both MMV688179 and MMV688362, however, are known to bind to the DNA minor groove, as shown by SPR, ITC, CD, and T_m experiments [78,85], which also correlates with the potency against *T. brucei*. Our findings regarding cruzain inhibition suggest, thus, a possible dual mechanism of action. To what extent the trypanocidal effect is derived from the cruzain or DNA binding effect is still to be evaluated by further studies. Finally, it is worth noting that multi-target drugs are an interesting strategy in medicinal chemistry, possibly leading to improved efficacy and overcoming drug resistance [86,87].

The overall hit rate of 1.5% (6 out of 400) observed in our screening was similar to the 1% (4 out of 400) hit rate against cruzain and *Tbr*CatL we reported upon screening MMV's Malaria Box [63]. PB was also screened against SARS-CoV-2 M^{Pro}, a cysteine protease from another family, yielding 2 hits (hit rate = 0.5%). Interestingly, MMV688179 was one of the hits with an IC_{50} of 1.6 μM against M^{Pro} [88]. As MMV688179 does not possess electrophilic moieties (see Figure 3), the M^{Pro} activity is likely due to specific interactions with the enzyme. This is also in line with the lack of MMV688179 inhibition against two unrelated human proteins ferrochelatase and porphobilinogen deaminase [89]. As the reported CC_{50} of MMV688179 is 11.6 μM [89], the selectivity towards the parasite is a clear focus of optimization rounds. It has been reported that cruzain inhibitors can show selectivity towards the parasite [47,51], suggesting that optimizing the cruzain potency of MMV688179 may be an attractive strategy for improving selectivity. Our hit rate is also in line, albeit the much smaller screening library, with the ones reported in HTS campaigns against cruzain (912 out of 197861, 0.46% [73]) and human cathepsin B (20 out of 64000, 0.03% [90]), a highly similar protein. In light of these observations, we believe that screening diverse, curated, yet concise, molecule libraries is an attractive strategy for discovering hits.

It is worth noting that here we report MMV688179 to be a novel, non-covalent cruzain inhibitor bearing a competitive mechanism and nanomolar potency. Unfortunately, we could not determine the potency of a first round of analogues due to interference of the small molecules with the assay readout. Nevertheless, MMV688179 is an interesting candidate for hit-to-lead optimization. This is also true, to a lesser extent, for MMV688362 and MMV687812 which inhibited cruzain and *Tbr*CatL in the 2–4 μM range.

In summary, three main contributions arise from this work. First, our results shed light on possible trypanocidal mechanisms of some of the PB compounds. Second, we add to the evidence that screening diverse and curated, yet small libraries are a useful strategy for discovering new leads. Third, we provide the drug discovery community with novel hits for drug discovery targeting cruzain and *Tbr*CatL.

5. Conclusions

CD and HAT remain relevant, life-threatening diseases affecting mainly disadvantaged populations worldwide. Here, we screened Pathogen Box against cruzain and *Tbr*CatL, two validated targets for discovering leads against *T. cruzi* and *T. brucei*, respectively. From the 400 compounds in the library, we obtained 12 hits and validated six of them as inhibitors of cruzain and *Tbr*CatL. Particularly, MMV687246 is a mixed inhibitor of cruzain with a K_i of 57 ± 6 μM and MMV688179 is a competitive inhibitor of cruzain with a K_i of 165 ± 63 nM. We also proposed a possible binding mode of MMV688179 to cruzain to aid further optimization efforts. Hit-to-lead optimization of MMV688179 should focus on increasing selectivity towards *T. cruzi* and improving its potency against cruzain may be an attractive strategy in that context. We believe that the molecules discovered in this work, especially MMV688179 are candidates for optimization.

References

1. Nussbaum, K.; Honek, J.; Cadmus, C.; Efferth, T. Trypanosomatid Parasites Causing Neglected Diseases. *Curr. Med. Chem.* **2010**, *17*, 1594–1617. [CrossRef] [PubMed]
2. Stanaway, J.D.; Gregory, R. *The Global Burden of Disease: Generating Evidence, Guiding Policy: European Union and European Free Trade Association Regional Edition*; Institute for Health Metrics and Evaluation: Seattle, WA, USA, 2013; ISBN 978-0-9840910-6-5.
3. Pinheiro, E.; Brum-Soares, L.; Reis, R.; Cubides, J.-C. Chagas Disease: Review of Needs, Neglect, and Obstacles to Treatment Access in Latin America. *Rev. Soc. Bras. Med. Trop.* **2017**, *50*, 296–300. [CrossRef]

4. Aksoy, S.; Buscher, P.; Lehane, M.; Solano, P.; Van Den Abbeele, J. Human African Trypanosomiasis Control: Achievements and Challenges. *PLoS Negl. Trop. Dis.* **2017**, *11*, e0005454. [CrossRef] [PubMed]

5. WHO Fact Sheet 259-Trypanosomiasis. Human African (Sleeping Sickness). Available online: http://www.who.int/mediacentre/factsheets/fs259/en/ (accessed on 8 December 2015).

6. Medone, P.; Ceccarelli, S.; Parham, P.E.; Figuera, A.; Rabinovich, J.E. The Impact of Climate Change on the Geographical Distribution of Two Vectors of Chagas Disease: Implications for the Force of Infection. *Philos. Trans. R. Soc. B Biol. Sci.* **2015**, *370*, 20130560. [CrossRef]

7. Molina, I.; Salvador, F.; Sánchez-Montalvá, A. Actualización en enfermedad de Chagas. *Enferm. Infecc. Microbiol. Clínica* **2016**, *34*, 132–138. [CrossRef]

8. Patrick, G.L. *An Introduction to Medicinal Chemistry*, 5th ed.; Oxford University Press: Oxford, UK, 2013; ISBN 978-0-19-969739-7.

9. Lenk, E.J.; Redekop, W.K.; Luyendijk, M.; Fitzpatrick, C.; Niessen, L.; Stolk, W.A.; Tediosi, F.; Rijnsburger, A.J.; Bakker, R.; Hontelez, J.A.C.; et al. Socioeconomic Benefit to Individuals of Achieving 2020 Targets for Four Neglected Tropical Diseases Controlled/Eliminated by Innovative and Intensified Disease Management: Human African Trypanosomiasis, Leprosy, Visceral Leishmaniasis, Chagas Disease. *PLoS Negl. Trop. Dis.* **2018**, *12*, e0006250. [CrossRef]

10. Bermudez, J.; Davies, C.; Simonazzi, A.; Pablo Real, J.; Palma, S. Current Drug Therapy and Pharmaceutical Challenges for Chagas Disease. *Acta Trop.* **2016**, *156*, 1–16. [CrossRef] [PubMed]

11. Ferreira, L.G.; Andricopulo, A.D. Targeting Cysteine Proteases in Trypanosomatid Disease Drug Discovery. *Pharmacol. Ther.* **2017**, *180*, 49–61. [CrossRef] [PubMed]

12. Rocha, D.A.; Silva, E.B.; Fortes, I.S.; Lopes, M.S.; Ferreira, R.S.; Andrade, S.F. Synthesis and Structure-Activity Relationship Studies of Cruzain and Rhodesain Inhibitors. *Eur. J. Med. Chem.* **2018**, *157*, 1426–1459. [CrossRef]

13. Caffrey, C.R.; Steverding, D.; Ferreira, R.S.; Oliveira, R.B.; O'Donoghue, A.J.; Monti, L.; Ballatore, C.; Bachovchin, K.A.; Ferrins, L.; Pollastri, M.P.; et al. Drug Discovery and Development for Kinetoplastid Diseases. In *Burger's Medicinal Chemistry and Drug Discovery*; Wiley: Hoboken, NJ, USA, 2021; pp. 1–79. ISBN 978-0-470-27815-4.

14. Morillo, C.A.; Marin-Neto, J.A.; Avezum, A.; Sosa-Estani, S.; Rassi, A.; Rosas, F.; Villena, E.; Quiroz, R.; Bonilla, R.; Britto, C.; et al. Randomized Trial of Benznidazole for Chronic Chagas' Cardiomyopathy. *N. Engl. J. Med.* **2015**, *373*, 1295–1306. [CrossRef]

15. Brun, R.; Blum, J.; Chappuis, F.; Burri, C. Human African Trypanosomiasis. *Lancet* **2010**, *375*, 148–159. [CrossRef] [PubMed]

16. Büscher, P.; Cecchi, G.; Jamonneau, V.; Priotto, G. Human African Trypanosomiasis. *Lancet* **2017**, *390*, 2397–2409. [CrossRef]

17. Fairlamb, A.H.; Horn, D. Melarsoprol Resistance in African Trypanosomiasis. *Trends Parasitol.* **2018**, *34*, 481–492. [CrossRef] [PubMed]

18. Pépin, J.; Khonde, N.; Maiso, F.; Doua, F.; Jaffar, S.; Ngampo, S.; Mpia, B.; Mbulamberi, D.; Kuzoe, F. Short-Course Eflornithine in Gambian Trypanosomiasis: A Multicentre Randomized Controlled Trial. *Bull. World Health Organ.* **2000**, *78*, 1284–1295. [PubMed]

19. Priotto, G.; Pinoges, L.; Fursa, I.B.; Burke, B.; Nicolay, N.; Grillet, G.; Hewison, C.; Balasegaram, M. Safety and Effectiveness of First Line Eflornithine for Trypanosoma Brucei Gambiense Sleeping Sickness in Sudan: Cohort Study. *BMJ* **2008**, *336*, 705–708. [CrossRef]

20. Priotto, G.; Kasparian, S.; Mutombo, W.; Ngouama, D.; Ghorashian, S.; Arnold, U.; Ghabri, S.; Baudin, E.; Buard, V.; Kazadi-Kyanza, S.; et al. Nifurtimox-Eflornithine Combination Therapy for Second-Stage African Trypanosoma Brucei Gambiense Trypanosomiasis: A Multicentre, Randomised, Phase III, Non-Inferiority Trial. *Lancet* **2009**, *374*, 56–64. [CrossRef]

21. Kuemmerle, A.; Schmid, C.; Bernhard, S.; Kande, V.; Mutombo, W.; Ilunga, M.; Lumpungu, I.; Mutanda, S.; Nganzobo, P.; Tete, D.N.; et al. Effectiveness of Nifurtimox Eflornithine Combination Therapy (NECT) in T. b. Gambiense Second Stage Sleeping Sickness Patients in the Democratic Republic of Congo: Report from a Field Study. *PLoS Negl. Trop. Dis.* **2021**, *15*, e0009903. [CrossRef]

22. Kansiime, F.; Adibaku, S.; Wamboga, C.; Idi, F.; Kato, C.D.; Yamuah, L.; Vaillant, M.; Kioy, D.; Olliaro, P.; Matovu, E. A Multi-centre, Randomised, Non-Inferiority Clinical Trial Comparing a Nifurtimox-Eflornithine Combination to Standard Eflornithine Monotherapy for Late Stage Trypanosoma Brucei Gambiense Human African Trypanosomiasis in Uganda. *Parasites Vectors* **2018**, *11*, 105. [CrossRef]

23. Pollastri, M.P. Fexinidazole: A New Drug for African Sleeping Sickness on the Horizon. *Trends Parasitol.* **2018**, *34*, 178–179. [CrossRef]

24. Kande Betu Kumesu, V.; Mutombo Kalonji, W.; Bardonneau, C.; Valverde Mordt, O.; Ngolo Tete, D.; Blesson, S.; Simon, F.; Delhomme, S.; Bernhard, S.; Nganzobo Ngima, P.; et al. Safety and Efficacy of Oral Fexinidazole in Children with Gambiense Human African Trypanosomiasis: A Multicentre, Single-Arm, Open-Label, Phase 2–3 Trial. *Lancet Glob. Health* **2022**, *10*, e1665–e1674. [CrossRef]

25. Lindner, A.K.; Lejon, V.; Chappuis, F.; Seixas, J.; Kazumba, L.; Barrett, M.P.; Mwamba, E.; Erphas, O.; Akl, E.A.; Villanueva, G.; et al. New WHO Guidelines for Treatment of Gambiense Human African Trypanosomiasis Including Fexinidazole: Substantial Changes for Clinical Practice. *Lancet Infect. Dis.* **2020**, *20*, e38–e46. [CrossRef] [PubMed]

26. Efficacy and Safety of Fexinidazole in Patients with Human African Trypanosomiasis (HAT) Due to Trypanosoma Brucei Rhodesiense. Available online: https://beta.clinicaltrials.gov/study/NCT03974178 (accessed on 20 December 2022).

27. Chen, Y.T.; Brinen, L.S.; Kerr, I.D.; Hansell, E.; Doyle, P.S.; McKerrow, J.H.; Roush, W.R. In Vitro and In Vivo Studies of the Trypanocidal Properties of WRR-483 against Trypanosoma Cruzi. *PLoS Negl. Trop. Dis.* **2010**, *4*, e825. [CrossRef] [PubMed]

28. Barr, S.C.; Warner, K.L.; Kornreic, B.G.; Piscitelli, J.; Wolfe, A.; Benet, L.; McKerrow, J.H. A Cysteine Protease Inhibitor Protects Dogs from Cardiac Damage during Infection by Trypanosoma Cruzi. *Antimicrob. Agents Chemother.* **2005**, *49*, 5160–5161. [CrossRef] [PubMed]

29. da Silva, E.B.; do Nascimento Pereira, G.A.; Ferreira, R.S. Trypanosomal Cysteine Peptidases: Target Validation and Drug Design Strategies. In *Comprehensive Analysis of Parasite Biology: From Metabolism to Drug Discovery*; Müller, S., Cerdan, R., Radulescu, O., Eds.; Wiley-VCH Verlag GmbH & Co. KGaA: Weinheim, Germany, 2016; pp. 121–145. ISBN 978-3-527-33904-4.

30. dos Santos Nascimento, I.J.; de Aquino, T.M.; da Silva-Júnior, E.F. Cruzain and Rhodesain Inhibitors: Last Decade of Advances in Seeking for New Compounds Against American and African Trypanosomiases. *Curr. Top. Med. Chem.* **2021**, *21*, 1871–1899. [CrossRef] [PubMed]

31. Santos, V.C.; Oliveira, A.E.R.; Campos, A.C.B.; Reis-Cunha, J.L.; Bartholomeu, D.C.; Teixeira, S.M.R.; Lima, A.P.C.A.; Ferreira, R.S. The Gene Repertoire of the Main Cysteine Protease of Trypanosoma Cruzi, Cruzipain, Reveals Four Sub-Types with Distinct Active Sites. *Sci. Rep.* **2021**, *11*, 18231. [CrossRef] [PubMed]

32. Alvarez, V.E.; Iribarren, P.A.; Niemirowicz, G.T.; Cazzulo, J.J. Update on Relevant Trypanosome Peptidases: Validated Targets and Future Challenges. *Biochim. Biophys. Acta BBA-Proteins Proteom.* **2021**, *1869*, 140577. [CrossRef]

33. Giroud, M.; Dietzel, U.; Anselm, L.; Banner, D.; Kuglstatter, A.; Benz, J.; Blanc, J.-B.; Gaufreteau, D.; Liu, H.; Lin, X.; et al. Repurposing a Library of Human Cathepsin L Ligands: Identification of Macrocyclic Lactams as Potent Rhodesain and Trypanosoma Brucei Inhibitors. *J. Med. Chem.* **2018**, *61*, 3350–3369. [CrossRef]

34. Eakin, A.E.; Mills, A.A.; Harth, G.; McKerrow, J.H.; Craik, C.S. The Sequence, Organization, and Expression of the Major Cysteine Protease (Cruzain) from Trypanosoma Cruzi. *J. Biol. Chem.* **1992**, *267*, 7411–7420. [CrossRef]

35. Harth, G.; Andrews, N.; Mills, A.A.; Engel, J.C.; Smith, R.; McKerrow, J.H. Peptide-Fluoromethyl Ketones Arrest Intracellular Replication and Intercellular Transmission of Trypanosoma Cruzi. *Mol. Biochem. Parasitol.* **1993**, *58*, 17–24. [CrossRef]

36. Meirelles, M.N.; Juliano, L.; Carmona, E.; Silva, S.G.; Costa, E.M.; Murta, A.C.; Scharfstein, J. Inhibitors of the Major Cysteinyl Proteinase (GP57/51) Impair Host Cell Invasion and Arrest the Intracellular Development of Trypanosoma Cruzi in Vitro. *Mol. Biochem. Parasitol.* **1992**, *52*, 175–184. [CrossRef]

37. Aparicio, I.M.; Scharfstein, J.; Lima, A.P.C.A. A New Cruzipain-Mediated Pathway of Human Cell Invasion by Trypanosoma Cruzi Requires Trypomastigote Membranes. *Infect. Immun.* **2004**, *72*, 5892–5902. [CrossRef]

38. Doyle, P.S.; Zhou, Y.M.; Hsieh, I.; Greenbaum, D.C.; McKerrow, J.H.; Engel, J.C. The Trypanosoma Cruzi Protease Cruzain Mediates Immune Evasion. *PLoS Pathog.* **2011**, *7*, e1002139. [CrossRef] [PubMed]

39. Lonsdale-Eccles, J.D.; Grab, D.J. Trypanosome Hydrolases and the Blood–Brain Barrier. *Trends Parasitol.* **2002**, *18*, 17–19. [CrossRef] [PubMed]

40. Mogk, S.; Boßelmann, C.M.; Mudogo, C.N.; Stein, J.; Wolburg, H.; Duszenko, M. African Trypanosomes and Brain Infection—The Unsolved Question: Brain Infection in African Sleeping Sickness. *Biol. Rev.* **2017**, *92*, 1675–1687. [CrossRef] [PubMed]

41. Du, X.; Guo, C.; Hansell, E.; Doyle, P.S.; Caffrey, C.R.; Holler, T.P.; McKerrow, J.H.; Cohen, F.E. Synthesis and Structure−Activity Relationship Study of Potent Trypanocidal Thio Semicarbazone Inhibitors of the Trypanosomal Cysteine Protease Cruzain. *J. Med. Chem.* **2002**, *45*, 2695–2707. [CrossRef]

42. Fonseca, N.C.; da Cruz, L.F.; da Silva Villela, F.; do Nascimento Pereira, G.A.; de Siqueira-Neto, J.L.; Kellar, D.; Suzuki, B.M.; Ray, D.; de Souza, T.B.; Alves, R.J.; et al. Synthesis of a Sugar-Based Thiosemicarbazone Series and Structure-Activity Relationship versus the Parasite Cysteine Proteases Rhodesain, Cruzain, and Schistosoma Mansoni Cathepsin B1. *Antimicrob. Agents Chemother.* **2015**, *59*, 2666–2677. [CrossRef] [PubMed]

43. Mott, B.T.; Ferreira, R.S.; Simeonov, A.; Jadhav, A.; Ang, K.K.-H.; Leister, W.; Shen, M.; Silveira, J.T.; Doyle, P.S.; Arkin, M.R.; et al. Identification and Optimization of Inhibitors of Trypanosomal Cysteine Proteases: Cruzain, Rhodesain, and TbCatB. *J. Med. Chem.* **2010**, *53*, 52–60. [CrossRef]

44. Alves, L.; Santos, D.A.; Cendron, R.; Rocho, F.R.; Matos, T.K.B.; Leitão, A.; Montanari, C.A. Nitrile-Based Peptoids as Cysteine Protease Inhibitors. *Bioorg. Med. Chem.* **2021**, *41*, 116211. [CrossRef]

45. Braga, S.F.P.; Martins, L.C.; da Silva, E.B.; Sales Júnior, P.A.; Murta, S.M.F.; Romanha, A.J.; Soh, W.T.; Brandstetter, H.; Ferreira, R.S.; de Oliveira, R.B. Synthesis and Biological Evaluation of Potential Inhibitors of the Cysteine Proteases Cruzain and Rhodesain Designed by Molecular Simplification. *Bioorg. Med. Chem.* **2017**, *25*, 1889–1900. [CrossRef]

46. Ferreira, R.S.; Dessoy, M.A.; Pauli, I.; Souza, M.L.; Krogh, R.; Sales, A.I.L.; Oliva, G.; Dias, L.C.; Andricopulo, A.D. Synthesis, Biological Evaluation, and Structure–Activity Relationships of Potent Noncovalent and Nonpeptidic Cruzain Inhibitors as Anti-Trypanosoma Cruzi Agents. *J. Med. Chem.* **2014**, *57*, 2380–2392. [CrossRef] [PubMed]

47. Pauli, I.; Rezende, C.D.O., Jr.; Slafer, B.W.; Dessoy, M.A.; de Souza, M.L.; Ferreira, L.L.G.; Adjanohun, A.L.M.; Ferreira, R.S.; Magalhães, L.G.; Krogh, R.; et al. Multiparameter Optimization of Trypanocidal Cruzain Inhibitors With In Vivo Activity and Favorable Pharmacokinetics. *Front. Pharmacol.* **2022**, *12*, 3570. [CrossRef] [PubMed]

48. Bryant, C.; Kerr, I.D.; Debnath, M.; Ang, K.K.H.; Ratnam, J.; Ferreira, R.S.; Jaishankar, P.; Zhao, D.; Arkin, M.R.; McKerrow, J.H.; et al. Novel Non-Peptidic Vinylsulfones Targeting the S2 and S3 Subsites of Parasite Cysteine Proteases. *Bioorg. Med. Chem. Lett.* **2009**, *19*, 6218–6221. [CrossRef]

49. Doyle, P.S.; Zhou, Y.M.; Engel, J.C.; McKerrow, J.H. A Cysteine Protease Inhibitor Cures Chagas' Disease in an Immunodeficient-Mouse Model of Infection. *Antimicrob. Agents Chemother.* **2007**, *51*, 3932–3939. [CrossRef] [PubMed]

50. Barbosa Da Silva, E.; Sharma, V.; Hernandez-Alvarez, L.; Tang, A.H.; Stoye, A.; O'Donoghue, A.J.; Gerwick, W.H.; Payne, R.J.; McKerrow, J.H.; Podust, L.M. Intramolecular Interactions Enhance the Potency of Gallinamide A Analogues against Trypanosoma Cruzi. *J. Med. Chem.* **2022**, *65*, 4255–4269. [CrossRef] [PubMed]

51. Barbosa da Silva, E.; Rocha, D.A.; Fortes, I.S.; Yang, W.; Monti, L.; Siqueira-Neto, J.L.; Caffrey, C.R.; McKerrow, J.; Andrade, S.F.; Ferreira, R.S. Structure-Based Optimization of Quinazolines as Cruzain and Tbr CATL Inhibitors. *J. Med. Chem.* **2021**, *64*, 13054–13071. [CrossRef]

52. de Souza, M.L.; de Oliveira Rezende Junior, C.; Ferreira, R.S.; Espinoza Chávez, R.M.; Ferreira, L.L.G.; Slafer, B.W.; Magalhães, L.G.; Krogh, R.; Oliva, G.; Cruz, F.C.; et al. Discovery of Potent, Reversible, and Competitive Cruzain Inhibitors with Trypanocidal Activity: A Structure-Based Drug Design Approach. *J. Chem. Inf. Model.* **2020**, *60*, 1028–1041. [CrossRef]

53. Greenbaum, D.C.; Mackey, Z.; Hansell, E.; Doyle, P.; Gut, J.; Caffrey, C.R.; Lehrman, J.; Rosenthal, P.J.; McKerrow, J.H.; Chibale, K. Synthesis and Structure−Activity Relationships of Parasiticidal Thiosemicarbazone Cysteine Protease Inhibitors against Plasmodium Falciparum, Trypanosoma Brucei, and Trypanosoma Cruzi. *J. Med. Chem.* **2004**, *47*, 3212–3219. [CrossRef]

54. Ettari, R.; Tamborini, L.; Angelo, I.C.; Grasso, S.; Schirmeister, T.; Lo Presti, L.; De Micheli, C.; Pinto, A.; Conti, P. Development of Rhodesain Inhibitors with a 3-Bromoisoxazoline Warhead. *ChemMedChem* **2013**, *8*, 2070–2076. [CrossRef]

55. Yang, P.-Y.; Wang, M.; Li, L.; Wu, H.; He, C.Y.; Yao, S.Q. Design, Synthesis and Biological Evaluation of Potent Azadipeptide Nitrile Inhibitors and Activity-Based Probes as Promising Anti—Trypanosoma Brucei Agents. *Chem.-Eur. J.* **2012**, *18*, 6528–6541. [CrossRef]

56. Mallari, J.P.; Shelat, A.A.; Obrien, T.; Caffrey, C.R.; Kosinski, A.; Connelly, M.; Harbut, M.; Greenbaum, D.; McKerrow, J.H.; Guy, R.K. Development of Potent Purine-Derived Nitrile Inhibitors of the Trypanosomal Protease TbcatB. *J. Med. Chem.* **2008**, *51*, 545–552. [CrossRef]

57. Kryshchyshyn, A.; Kaminskyy, D.; Karpenko, O.; Gzella, A.; Grellier, P.; Lesyk, R. Thiazolidinone/Thiazole Based Hybrids–New Class of Antitrypanosomal Agents. *Eur. J. Med. Chem.* **2019**, *174*, 292–308. [CrossRef] [PubMed]

58. Havrylyuk, D.; Zimenkovsky, B.; Vasylenko, O.; Day, C.W.; Smee, D.F.; Grellier, P.; Lesyk, R. Synthesis and Biological Activity Evaluation of 5-Pyrazoline Substituted 4-Thiazolidinones. *Eur. J. Med. Chem.* **2013**, *66*, 228–237. [CrossRef]

59. Silva, F.T.; Franco, C.H.; Favaro, D.C.; Freitas-Junior, L.H.; Moraes, C.B.; Ferreira, E.I. Design, Synthesis and Antitrypanosomal Activity of Some Nitrofurazone 1,2,4-Triazolic Bioisosteric Analogues. *Eur. J. Med. Chem.* **2016**, *121*, 553–560. [CrossRef] [PubMed]

60. Kerr, I.D.; Lee, J.H.; Farady, C.J.; Marion, R.; Rickert, M.; Sajid, M.; Pandey, K.C.; Caffrey, C.R.; Legac, J.; Hansell, E.; et al. Vinyl Sulfones as Antiparasitic Agents and a Structural Basis for Drug Design. *J. Biol. Chem.* **2009**, *284*, 25697–25703. [CrossRef]

61. Ettari, R.; Previti, S.; Maiorana, S.; Amendola, G.; Wagner, A.; Cosconati, S.; Schirmeister, T.; Hellmich, U.A.; Zappalà, M. Optimization Strategy of Novel Peptide-Based Michael Acceptors for the Treatment of Human African Trypanosomiasis. *J. Med. Chem.* **2019**, *62*, 10617–10629. [CrossRef]

62. Previti, S.; Ettari, R.; Di Chio, C.; Ravichandran, R.; Bogacz, M.; Hellmich, U.A.; Schirmeister, T.; Cosconati, S.; Zappalà, M. Development of Reduced Peptide Bond Pseudopeptide Michael Acceptors for the Treatment of Human African Trypanosomiasis. *Molecules* **2022**, *27*, 3765. [CrossRef] [PubMed]

63. Pereira, G.A.N.; da Silva, E.B.; Braga, S.F.P.; Leite, P.G.; Martins, L.C.; Vieira, R.P.; Soh, W.T.; Villela, F.S.; Costa, F.M.R.; Ray, D.; et al. Discovery and Characterization of Trypanocidal Cysteine Protease Inhibitors from the 'Malaria Box'. *Eur. J. Med. Chem.* **2019**, *179*, 765–778. [CrossRef]

64. Silva, L.R.; Guimarães, A.S.; do Nascimento, J.; do Santos Nascimento, I.J.; da Silva, E.B.; McKerrow, J.H.; Cardoso, S.H.; da Silva-Júnior, E.F. Computer-Aided Design of 1,4-Naphthoquinone-Based Inhibitors Targeting Cruzain and Rhodesain Cysteine Proteases. *Bioorg. Med. Chem.* **2021**, *41*, 116213. [CrossRef]

65. Van Voorhis, W.C.; Adams, J.H.; Adelfio, R.; Ahyong, V.; Akabas, M.H.; Alano, P.; Alday, A.; Alemán Resto, Y.; Alsibaee, A.; Alzualde, A.; et al. Open Source Drug Discovery with the Malaria Box Compound Collection for Neglected Diseases and Beyond. *PLoS Pathog.* **2016**, *12*, e1005763. [CrossRef]

66. Duffy, S.; Sykes, M.L.; Jones, A.J.; Shelper, T.B.; Simpson, M.; Lang, R.; Poulsen, S.-A.; Sleebs, B.E.; Avery, V.M. Screening the Medicines for Malaria Venture Pathogen Box across Multiple Pathogens Reclassifies Starting Points for Open-Source Drug Discovery. *Antimicrob. Agents Chemother.* **2017**, *61*, e00379-17. [CrossRef]

67. Veale, C.G.L.; Laming, D.; Swart, T.; Chibale, K.; Hoppe, H.C. Exploring the Antiplasmodial 2-Aminopyridines as Potential Antitrypanosomal Agents. *ChemMedChem* **2019**, *14*, 2034–2041. [CrossRef] [PubMed]

68. Gaulton, A.; Hersey, A.; Nowotka, M.; Bento, A.P.; Chambers, J.; Mendez, D.; Mutowo, P.; Atkinson, F.; Bellis, L.J.; Cibrián-Uhalte, E.; et al. The ChEMBL Database in 2017. *Nucleic Acids Res.* **2017**, *45*, D945–D954. [CrossRef]

69. Veríssimo, G.C.; dos Santos Júnior, V.S.; de Almeida, I.A.D.R.; Ruas, M.S.M.; Coutinho, L.G.; de Oliveira, R.B.; Alves, R.J.; Maltarollo, V.G. The Brazilian Compound Library (BraCoLi) Database: A Repository of Chemical and Biological Information for Drug Design. *Mol. Divers.* **2022**, *26*, 3387–3397. [CrossRef]

70. Bemis, G.W.; Murcko, M.A. The Properties of Known Drugs. 1. Molecular Frameworks. *J. Med. Chem.* **1996**, *39*, 2887–2893. [CrossRef]

71. de Oliveira, R.B.; Vaz, A.B.; Alves, R.O.; Liarte, D.B.; Donnici, C.L.; Romanha, A.J.; Zani, C.L. Arylfurans as Potential Trypanosoma Cruzi Trypanothione Reductase Inhibitors. *Mem. Inst. Oswaldo Cruz* **2006**, *101*, 169–173. [CrossRef]

72. Oliveira, R.B.D.; Zani, C.L.; Ferreira, R.S.; Leite, R.S.; Alves, T.M.A.; da Silva, T.H.A.; Romanha, A.J. Síntese, Avaliação Biológica e Modelagem Molecular de Arilfuranos Como Inibidores Da Enzima Tripanotiona Redutase. *Quím. Nova* **2008**, *31*, 261–267. [CrossRef]

73. Ferreira, R.S.; Simeonov, A.; Jadhav, A.; Eidam, O.; Mott, B.T.; Keiser, M.J.; McKerrow, J.H.; Maloney, D.J.; Irwin, J.J.; Shoichet, B.K. Complementarity Between a Docking and a High-Throughput Screen in Discovering New Cruzain Inhibitors. *J. Med. Chem.* **2010**, *53*, 4891–4905. [CrossRef]

74. Dolinsky, T.J.; Nielsen, J.E.; McCammon, J.A.; Baker, N.A. PDB2PQR: An Automated Pipeline for the Setup of Poisson-Boltzmann Electrostatics Calculations. *Nucleic Acids Res.* **2004**, *32*, W665–W667. [CrossRef]

75. Turney, J.M.; Simmonett, A.C.; Parrish, R.M.; Hohenstein, E.G.; Evangelista, F.A.; Fermann, J.T.; Mintz, B.J.; Burns, L.A.; Wilke, J.J.; Abrams, M.L.; et al. Psi4: An Open-Source Ab Initio Electronic Structure Program: Psi4: An Electronic Structure Program. *Wiley Interdiscip. Rev. Comput. Mol. Sci.* **2012**, *2*, 556–565. [CrossRef]

76. Trott, O.; Olson, A.J. AutoDock Vina: Improving the Speed and Accuracy of Docking with a New Scoring Function, Efficient Optimization and Multithreading. *J. Comput. Chem.* **2010**, *31*, 455–461. [CrossRef] [PubMed]

77. Veale, C.G.L. Unpacking the Pathogen Box—An Open Source Tool for Fighting Neglected Tropical Disease. *ChemMedChem* **2019**, *14*, 386–453. [CrossRef] [PubMed]

78. Rodríguez, F.; Rozas, I.; Kaiser, M.; Brun, R.; Nguyen, B.; Wilson, W.D.; García, R.N.; Dardonville, C. New Bis(2-Aminoimidazoline) and Bisguanidine DNA Minor Groove Binders with Potent in Vivo Antitrypanosomal and Antiplasmodial Activity. *J. Med. Chem.* **2008**, *51*, 909–923. [CrossRef] [PubMed]

79. Jadhav, A.; Ferreira, R.S.; Klumpp, C.; Mott, B.T.; Austin, C.P.; Inglese, J.; Thomas, C.J.; Maloney, D.J.; Shoichet, B.K.; Simeonov, A. Quantitative Analyses of Aggregation, Autofluorescence, and Reactivity Artifacts in a Screen for Inhibitors of a Thiol Protease. *J. Med. Chem.* **2010**, *53*, 37–51. [CrossRef] [PubMed]

80. McGovern, S.L.; Caselli, E.; Grigorieff, N.; Shoichet, B.K. A Common Mechanism Underlying Promiscuous Inhibitors from Virtual and High-Throughput Screening. *J. Med. Chem.* **2002**, *45*, 1712–1722. [CrossRef] [PubMed]

81. Coan, K.E.D.; Shoichet, B.K. Stability and Equilibria of Promiscuous Aggregates in High Protein Milieus. *Mol. Biosyst.* **2007**, *3*, 208–213. [CrossRef]

82. Aulner, N.; Danckaert, A.; Ihm, J.; Shum, D.; Shorte, S.L. Next-Generation Phenotypic Screening in Early Drug Discovery for Infectious Diseases. *Trends Parasitol.* **2019**, *35*, 559–570. [CrossRef]

83. Wall, R.J.; Carvalho, S.; Milne, R.; Bueren-Calabuig, J.A.; Moniz, S.; Cantizani-Perez, J.; MacLean, L.; Kessler, A.; Cotillo, I.; Sastry, L.; et al. The Q$_i$ Site of Cytochrome b Is a Promiscuous Drug Target in Trypanosoma Cruzi and Leishmania Donovani. *ACS Infect. Dis.* **2020**, *6*, 515–528. [CrossRef]

84. Stephens, C.E.; Brun, R.; Salem, M.M.; Werbovetz, K.A.; Tanious, F.; Wilson, W.D.; Boykin, D.W. The Activity of Diguanidino and 'Reversed' Diamidino 2,5-Diarylfurans versus Trypanosoma Cruzi and Leishmania Donovani. *Bioorg. Med. Chem. Lett.* **2003**, *13*, 2065–2069. [CrossRef]

85. Nagle, P.S.; Rodriguez, F.; Nguyen, B.; Wilson, W.D.; Rozas, I. High DNA Affinity of a Series of Peptide Linked Diaromatic Guanidinium-like Derivatives. *J. Med. Chem.* **2012**, *55*, 4397–4406. [CrossRef]

86. Prati, F.; Uliassi, E.; Bolognesi, M.L. Two Diseases, One Approach: Multitarget Drug Discovery in Alzheimer's and Neglected Tropical Diseases. *MedChemComm* **2014**, *5*, 853–861. [CrossRef]

87. Previti, S.; Di Chio, C.; Ettari, R.; Zappalà, M. Dual Inhibition of Parasitic Targets: A Valuable Strategy to TreatMalaria and Neglected Tropical Diseases. *Curr. Med. Chem.* **2022**, *29*, 2952–2978. [CrossRef] [PubMed]

88. Breidenbach, J.; Lemke, C.; Pillaiyar, T.; Schäkel, L.; Al Hamwi, G.; Diett, M.; Gedschold, R.; Geiger, N.; Lopez, V.; Mirza, S.; et al. Targeting the Main Protease of SARS-CoV-2: From the Establishment of High Throughput Screening to the Design of Tailored Inhibitors. *Angew. Chem. Int. Ed.* **2021**, *60*, 10423–10429. [CrossRef] [PubMed]

89. Ehmann, A. The Australian National University Dept of Immunology Pathogen Box Compounds Screened. Available online: https://www.ebi.ac.uk/chembl/doc/inspect/CHEMBL3987221 (accessed on 6 January 2023).

90. Motlekar, N.; Diamond, S.L.; Napper, A.D. Evaluation of an Orthogonal Pooling Strategy for Rapid High-Throughput Screening of Proteases. *ASSAY Drug Dev. Technol.* **2008**, *6*, 395–405. [CrossRef] [PubMed]